VELOCITY-PRESSURE CORRELATION MEASUREMENT USING VARIOUS STATIC-PRESSURE PROBES IN A WAKE OF A CIRCULAR CYLINDER

Takuya Kawata[*1], **Yoshitsugu Naka**[*2], **Koji Fukagata**[*1], **Shinnosuke Obi**[*1]

[*1]Department of MechanicalEngineering
Keio University
Hiyoshi 3-14-1, Kohoku-ku, Yokohama-shi 223-5866, Kanagawa, Japan
email: slowhand@z7.keio.jp (T. Kawata)

[*2]Laboratoire de Mécanique de Lille
Boulevard Paul Langevin 59655 Villeneuve d′Ascq Cédex, Lille, France

ABSTRACT

In the present study, an experimental investigation is conducted into the effect of the shape of a miniature static-pressure probe on the velocity-pressure correlation measurement. Ten static-pressure probes, with systematically-changed probe diameters and lengths, are compared in combination with an X-type hot-wire probe to examine the accuracy of the simultaneous measurement of the fluctuating velocity and pressure. The effect of the probe shape on the distance between the probes, which is necessary to avoid interference, is also investigated for the various pressure probes, and it is found that the change in probe diameter has the primary influence on the probe interference. In the velocity-pressure correlation measurements, the results of the pressure fluctuation p' and the velocity-pressure correlation $\overline{up}$ are not affected by the probe shape. On the other hand, it is indicated that the measurement of $\overline{vp}$ is extremely sensitive to the configuration of the pressure holes including its orientation.

INTRODUCTION

The velocity-pressure correlation is one of the important properties in describing turbulent flows; it plays a significant role in the transport of the kinetic turbulent energy in the flow regions involving large-scale vortex motions (Kawata et al., 2010; Yao et al., 2001), and also can be used for experimental eduction of vortex structures (Sakai et al., 2007).

Attempts for the measurement of the velocity-pressure correlation have been reported by several researchers including the authors′ research group (Naka et al., 2006, 2009; Sakai et al., 2007; Tsuji et al., 2007) using a hot-wire probe and a miniature static-pressure probe (SP-probe) which was originally developed by Toyoda et al. (1994). In this measurement method, a hot-wire probe and the SP-probe are placed adjacent to each other in order to obtain the fluctuating velocity and pressure at a single point simultaneously. Although the distance between the SP-probe and the hot-wire probe should

be as small as possible to achieve the sufficient spatial resolution, there should be some distance between the probes in order to avoid interference.

The shape of the SP-probe has an effect on some aspects of the measurement: On the frequency and directional response of the SP-probe in the fluctuating pressure measurement, and on the optimal distance between the probes in the velocity-pressure correlation measurement. Hence, the effect on the probe interference should be taken into account for the choice of the shape of the SP-probe used in the velocity-pressure correlation measurement. However, the effect of the probe shape on the velocity-pressure correlation measurement has not been investigated in contrast with the effect on the frequency and directional response, which have been well investigated, e.g. by Ishida et al. (1995).

In the present study, a systematic examination on the geometrical configuration of the SP-probe is conducted aiming at the further improvement of the quality of the simultaneous measurement of fluctuating velocity and pressure. Various SP-probes with different shape are employed and the interference between a hot-wire probe is investigated in a wake of a circular cylinder. Finally, the velocity-pressure correlation measurements are performed and the results measured by the various SP-probes are compared.

EXPERIMENT
Static-pressure probe

The parameters and a schematic of the SP-probes employed in the present study are shown in Table 1 and Fig. 1, respectively. The SP-probe consists of a thin pipe with a circular cone on its tip, and four small holes are placed on the surface separated by $90°$. There are ten SP-probes with different d, L_1 and L_2, where d is the outer diameter and L_1 and L_2 are the lengths from the pressure hole on the surface of the SP-probe to the tip and to the connection to the flare part, respectively. The thickness of the SP-probe and the diameter of

Table 1. List of SP-probes (dimensions in mm)

No.	d	L_1	L_2	No.	d	L_1	L_2
1	0.5	7.5	15.0	6	0.5	10	12.5
2	0.5	10	15.0	7	0.5	10	17.5
3	0.5	12.5	15.0	8	0.7	12	20
4	0.5	15	15.0	9	0.7	17	20
5	0.5	17.5	15.0	10	1.0	19.5	24.0
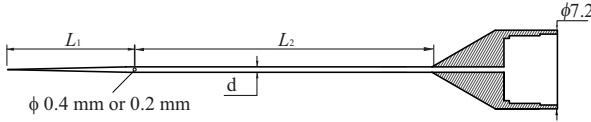
Figure 1. Schematics of SP-probe

Figure 2. Directional response of SP-probes

the pressure holes are 0.2 mm and 0.4 mm for the probe 10, and are 0.1 mm and 0.2 mm for the other probes. Note that the probe 10 has the same dimensions as that proposed by Toyoda et al. (1994) and the other probes have smaller dimensions.

The frequency and directional responses were investigated prior to the experiments. The frequency response was calibrated in the same manner as e.g. Naka et al. (2006), and the amplitude and the phase of the fluctuating pressure were corrected in the post processing. The directional responses of the various SP-probes were tested in a grid turbulence. The pressure fluctuation was measured by the SP-probes with various angles of attack of the mean flow, ϕ. The variation of the measured rms of the pressure fluctuation p' with ϕ are shown in Fig. 2. The values of p' are scaled by the value of p' with $\phi = 0°$. The SP-probes show the almost same response in $-20° < \phi < 20°$, and the difference can be seen in $|\phi| > 20°$ although the dependency on the probe shape is unclear. It should be noted that some SP-probes indicate asymmetric profiles with respect to $\phi = 0°$.

Experimental setup

Experiments were undertaken in a free stream of an opened blowing wind-tunnel. A circular cylinder with the diameter D of 10 mm was placed in a free stream, and the coordinate system was defined as shown in Fig. 3(a); the origin was placed at the center of the cylinder, and $x-$, $y-$ and $z-$ axes were taken in the streamwise, transverse and spanwise direction. The free steam velocity U_∞ was adjusted to be 6 m/s, and the Reynolds number, $Re = U_\infty D/\nu$, was 3900.

For the velocity measurements, an X-type hot-wire probe (X-probe; 55P64, Dantec) was employed and was combined with a constant temperature anemometer (CTA; Model 1011, Kanomax). For the fluctuating pressure measurement, the SP-probes were connected to a condenser microphone (UC-29, Rion) and the signal was amplified by the pre-amp (NH-05, Rion) and the main-amp (UN-04, Rion).

In the velocity-pressure correlation measurements, the X-probe and the SP-probe were placed as shown in Fig. 3(b),
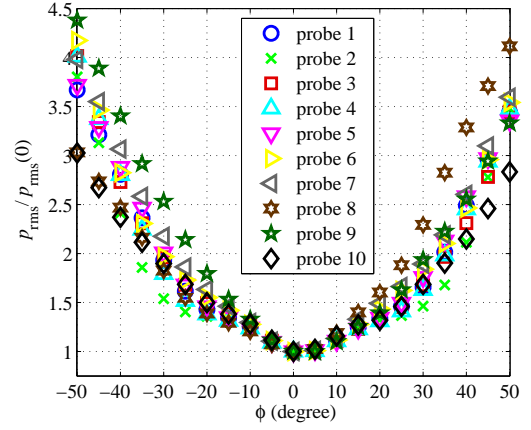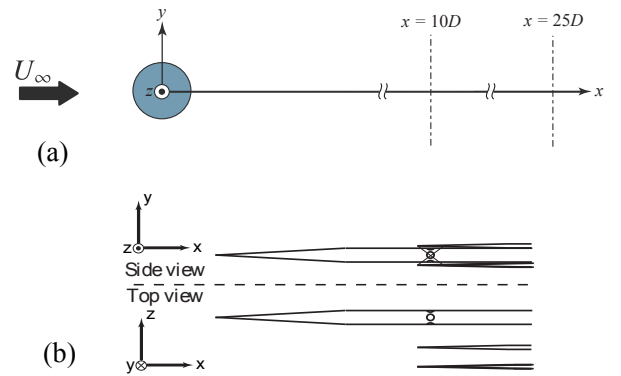

Figure 3. Experiment condition; (a) coodinate system, (b) probe configuration

and two instantaneous velocity components and fluctuating pressure were measured simultaneously.

Experimental Results

Probe Interference The effect of the probe interference was investigated for the various SP-probes. The X-probe and the SP-probe were placed at $(x, y) = (10D, -0.5D)$ and the velocity and pressure were measured simultaneously with spanwise different probe distances Δz. Note that the probes 6 and 7 were not used because the difference in L_2 is considered not to affect the probe interference.

Figure 4 shows the variation with Δz of the measured Reynolds stresses $\overline{v^2}$, $\overline{uv}$ and the velocity-pressure correlation coefficient $R_{vp} = \overline{vp}/(v'p')$, where the values of $\overline{v^2}$ and $\overline{uv}$ are scaled by the reference value separately measured by the X-probe and the SP-probe without interference. The variations of $\overline{v^2}$ and $\overline{uv}$ indicate that the interference between the SP-probe and the X-probe mainly depends on the probe diameter and does not on the length L_1. On the other hand, $R_{\overline{vp}}$ takes different values for the different probes. Based on these results, the optimal probe distance Δz is determined to be 3.0 mm for probes 1 to 7, and to be 4.0 mm for probes 8 to 10.
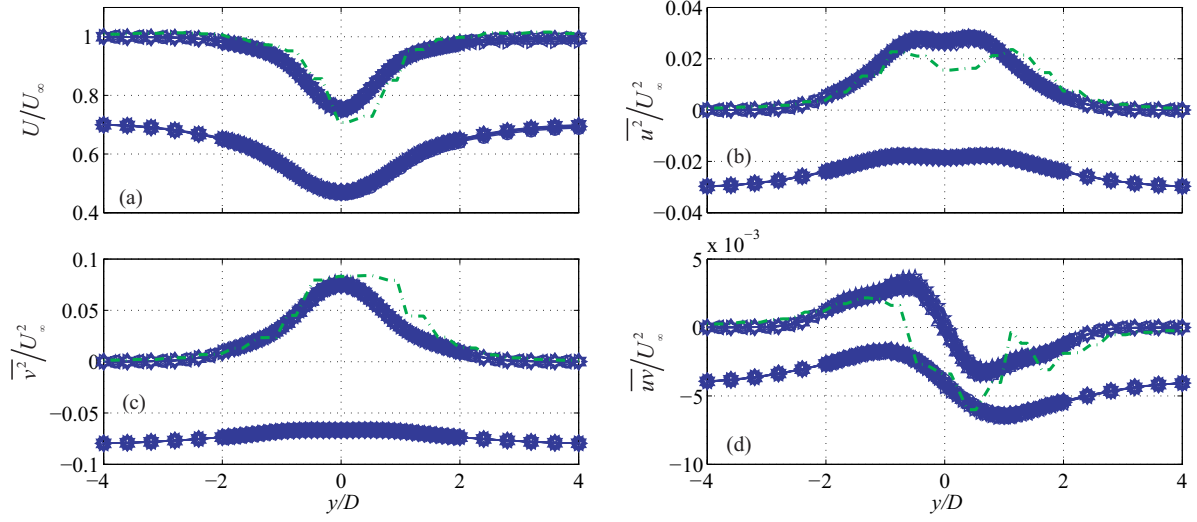
2

Figure 6. Mean streamwise velocity and Reynolds stresses at $x = 10D$ and $25D$ as top to bottom: experiments, various blue plots; LES (at $x = 10D$), green dashed line
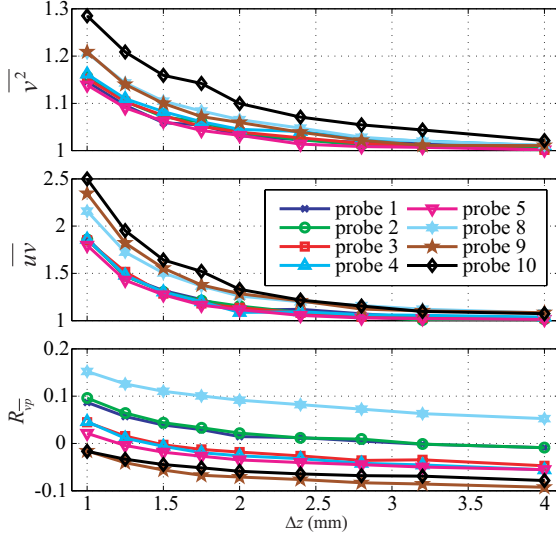

Figure 4. Effect of probe interference

Figure 5. Two-points correlation function in z direction measured at $x = 10D$ and $25D$

Velocity-Pressure Correlation Measurement The velocity-pressure correlation measurements were performed with the probe distance determined in the previous subsection. In order to investigate the performance of the SP-probes in flow regions with high and low turbulence intensities, the measurements were undertaken at two downstream locations in the wake of the circular cylinder; the relatively near region of the cylinder, $x = 10D$, and the further downstream location, $x = 25D$.

The profiles of the mean streamwise velocity and the Reynolds stresses measured by the X-probe with the various SP-probes are plotted together in Fig. 6 with the results of a large-eddy simulation (LES), which is described in the next section. The measured velocity profiles are in good agreement, indicating that the probe interference is avoided. The Reynolds normal stresses $\overline{u^2}$ and $\overline{v^2}$ dramatically decrease from $x = 10D$ to $x = 25D$, although the Reynolds shear stress $\overline{uv}$ does not show difference as much. At the center of the wake, $\overline{v^2}$ are 0.074 and 0.014 at $x = 10D$ and $25D$, respectively, corresponding to the attack angle fluctuation of the velocity vector to the probes of $15°$ and $6.8°$.

Pressure fluctuation p' and the velocity-pressure correla-

As previously described, the correlation between the fluctuating velocity and pressure at a single point is measured using two probes spatially separated by distance of 3.0 mm or 4.0 mm. In order to address the appropriateness of the present velocity-pressure correlation measurement, the two-point correlation measurements were performed and the integral scales of the flow field were evaluated. Figure 5 shows the measured auto-correlation functions, $R_{uu}(\Delta z) = \overline{u(z)u(z+\Delta z)}/\overline{u^2}(z)$. Integrating $R_{uu}(\Delta z)$ with respect to Δz, the integral scale was evaluated as $\Lambda = 6.50$ mm and 4.87 mm at $x = 10D$ and $25D$, respectively. Hence, the probe distance is in the same order of the integral scales. From Fig. 5, R_{uu} with Δz of 3.0 mm and 4.0 mm are calculated to be between 0.5 and 0.6. Therefore, the velocity-pressure correlation may be underestimated by 40-50 % in the present experiments.
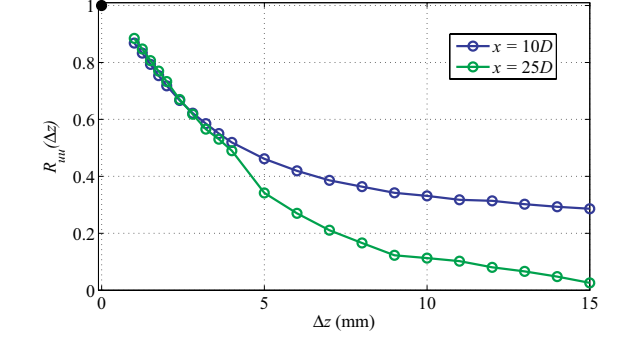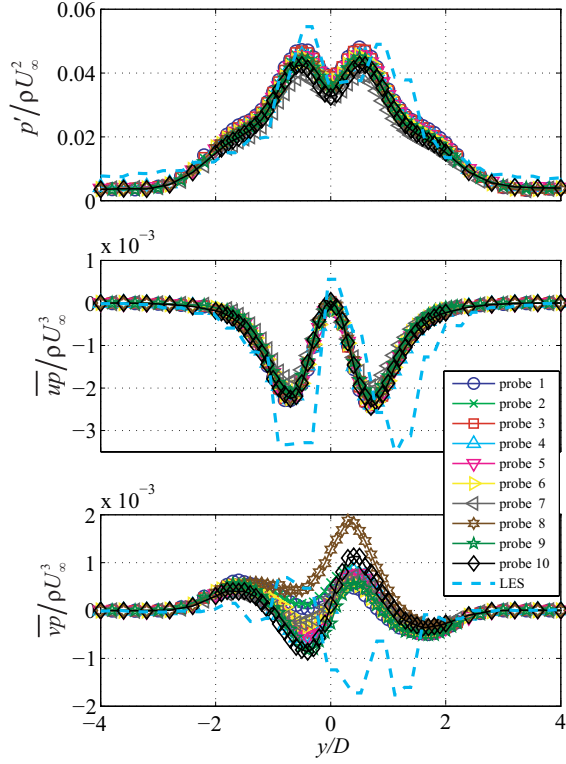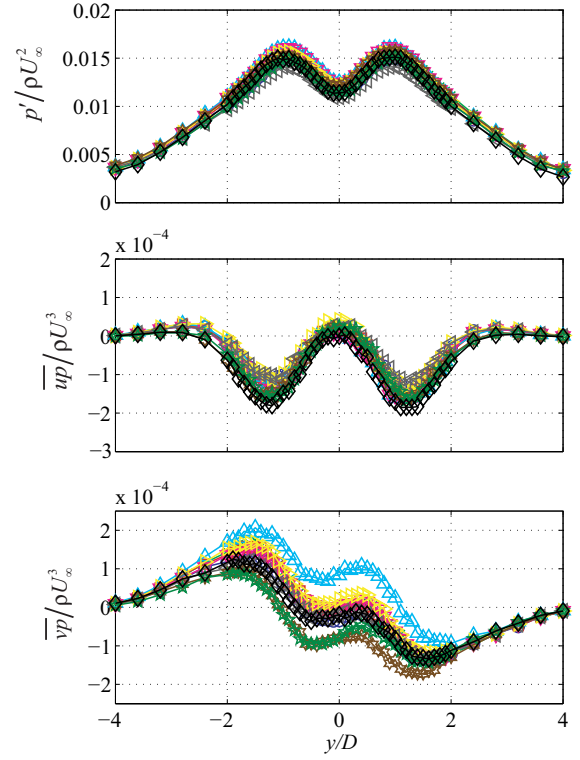
3

(a) At $x = 10D$

(b) At $x = 25D$ (symbols are same as shown in (a))

Figure 7. The distribution of pressure fluctuation p' and the velocity-pressure correlation $\overline{up}$ and $\overline{up}$ measured using various SP-probes

tion $\overline{up}$ and $\overline{vp}$ measured at $x = 10D$ and $x = 25D$ are shown in Fig. 7, and the LES results for $x = 10D$ are also plotted together. The profiles of p' and $\overline{up}$ measured using the various SP-probes are in fairly good agreement, which indicates that the measurement of p' and $\overline{up}$ is not affected by the difference in the probe shape. On the other hand, $\overline{vp}$ profiles show discrepancy, but the systematical relationship with the parameters, d, L_1 and L_2, cannot be found. It should be noted that these tendency in the performance of the SP-probes can be commonly seen in both of the downstream locations regardless of the turbulence intensity.

COMPUTATION
Computational Details

An LES was performed to obtain additional data of the velocity-pressure correlation for the validation of the experimental results. An open-source CFD software, OpenFOAM (http://www.openfoam.org), was used for the simulation. The Smagorinsky model was used as the subgrid scale model, and the Spalding law was adopted for the evaluation of the eddy viscosity at computational points adjacent to the wall.

The computational domain has a cylindrical shape with the radius of $15D$ and the spanwise size of πD. The number of grids in the radial, circumferential and spanwise direction were 166, 166, and 49.
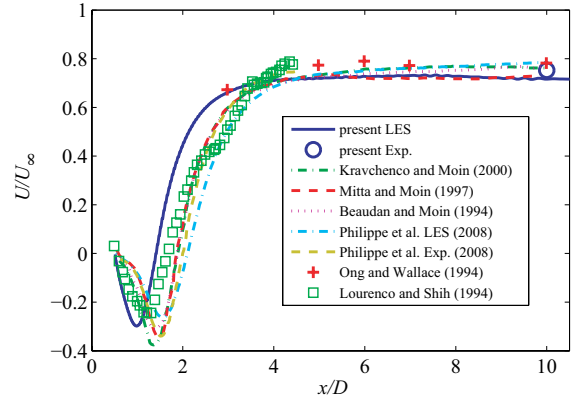

Figure 8. Mean streamwise velocity distribution along the center line

Computational Results

Figure 8 presents the distribution of the mean streamwise velocity along the centerline obtained from the present LES compared with other LESes and experiments. For the prediction of the near field, the present LES somewhat underestimates the length of recirculating region and predicts the recovery of the steamwise velocity earlier than the other study. On the other hand, in the downstream region ($x > 5D$), the
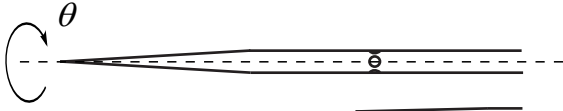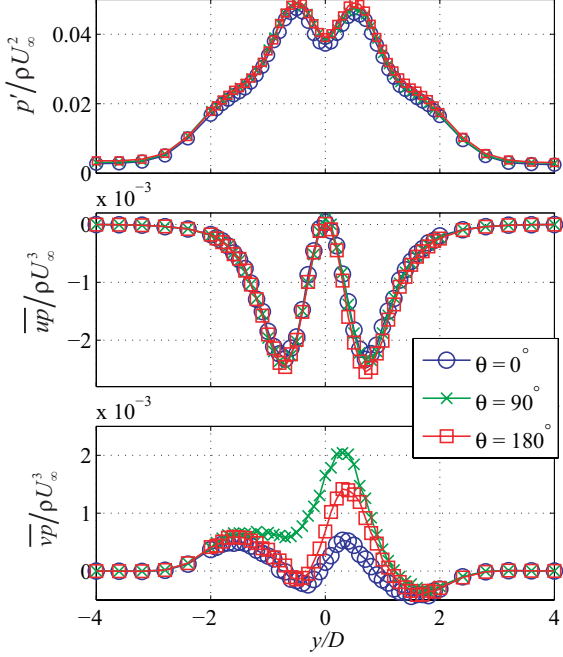
4

Figure 9. Rotation of SP-probe

Figure 10. Pressure-related statistics measured at $x = 10D$ using probe 8 with different θ

Figure 11. Power spectra measured at $(x, y) = (10D, 0D)$: (a), blue line, u; green line, v; (b) blue line, $\theta = 0°$; green line, $\theta = 90°$; red line, $\theta = 180°$

Figure 12. Cross spectra between v and p at $(x, y) = (10D, 0D)$ (colors are same as shown in Fig. 11(b))

present LES is in fairly good agreement with the other simulations and experiments.

As already shown in Fig. 6, the present LES satisfactorily predicts the streamwise velocity and the Reynolds normal stresses measured at $x = 10D$, although there is still discrepancy between the experiment and the LES in the profile of the Reynolds shear stress.

Figure 7(a) shows that p' and $\overline{up}$ provided by the present LES shown are in acceptable agreement with those measured in the present experiments. This partly supports the validity of the present measurement of p' and $\overline{up}$. On the other hand, the disagreement can be seen in $\overline{vp}$ provided by the present LES and by the measurements.

DISSCUSION

As mentioned in the section of experiment, discrepancy is indicated between $\overline{vp}$ measured by the various SP-probes while p' and $\overline{up}$ are in the good agreement, but the causal connection with the probe shape is unclear. In order to shed light on the cause of this discrepancy, the velocity-pressure correlation measurements were repeated rotating the SP-probe around its axis as schematically shown in Fig. 9: changing the position of the pressure hole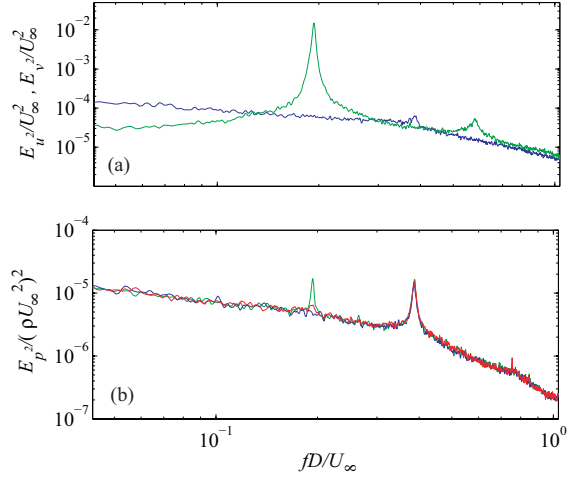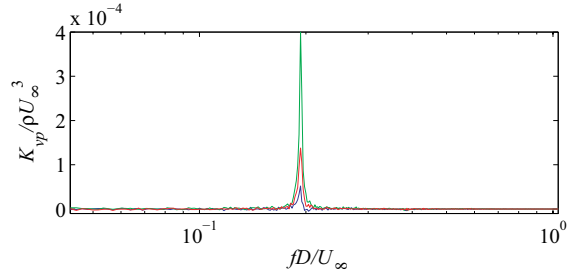s without yawing and pitching the SP-probe. Figure 10 shows the distributions of the pressure-related statistics measured using the probe 8 at $x = 10D$ with different θ, where θ is the rotation angle. It is indicated that the measurements of p' and $\overline{up}$ are not influenced by the direction of the pressure holes, but the measured distributions of $\overline{vp}$ shows significantly different profiles; it is almost symmetric in the case of $\theta = 0°$, but the profiles are shifted to the positive side in the cases of $\theta = 90°$, or $180°$.

Hereafter, the discussion is focused on the center of the wake as the representative point, and the spectral contents are investigated. Figure 11 presents the power spectra of fluctuating velocity and pressure. In Fig. 11(a), the spectrum of v shows a significant peak at $f = 0.19U_\infty/D$, while the spectrum of u shows a small peak at $f = 0.37U_\infty/D$. These peaks of velocity fluctuation are due to the Kármán vortex shedding. The spectra of p measured with different θ are compared in Fig. 11(b). All the spectra indicate peaks at $f = 0.37U_\infty/D$ as the spectrum of u. On the other hand, the difference can be seen at $f = 0.19U_\infty/D$: in the case of $\theta = 90°$ and $180°$, the slight peaks can be seen; in the case of $\theta = 0°$, no peak appears.

Figure 12 presents the real part of the cross spectra between v and p. A significant spike appears at $f = 0.19U_\infty/D$ in the cases of $\theta = 90°$ and $180°$, while the peak shown in the case of $\theta = 0°$ is small. The significant spikes of the cor-

5

relation in the case of $\theta = 90°$ and $180°$ are due to existence of the peaks of the spectrum of p, shown in Fig. 11, at the frequency where the significant peak of the spectrum of v exists. The different peak values of cross spectra result in the different values of $\overline{vp}$ at $y = 0D$ in Fig. 10.

Since four pressure holes are placed by $90°$ on the surface of the SP-probe, in $\theta = 0°, 90°$ and $180°$, the four pressure holes are just replaced to each other. Hence, the difference in the distributions of $\overline{vp}$ and the spectral contents may be attributed to the difference in the pressure hole diameters or the deviation of the hole positions from axisymmetric arrangement due to the working error in the manufacture of the SP-probes. The effect of such factors may also be seen in the asymmetric profiles of directional response of some of the SP-probe shown in Fig. 2, and the discrepancy in the distributions of the $\overline{vp}$ indicated in Fig. 7 may arise due to the same cause rather than the difference in the parameters of the probe shape.

CONCLUDING REMARKS

In the present study, a systematical investigation into the effect of the shape of the SP-probe on the velocity-pressure correlation measurement was conducted by comparing the performances of the SP-probes with various probe shapes. In the investigation of the interference between the pressure probe and a hot-wire probe, it is revealed that the optimal probe distance mainly depends on the probe diameter and does not on the length. In the velocity-pressure correlation measurement, it is indicated that the difference in the probe shape does not affect the measurement of pressure fluctuation p' and the velocity-pressure correlation $\overline{up}$, and the measured p' and $\overline{up}$ are in fairly good agreement with those provided by a large-eddy simulation. On the other hand, the velocity-pressure correlation $\overline{vp}$ measured by the various probes disagree with each other, although any causal relationship with the probe shape is not observed. It is indicated by the extra experiments that the measurement of $\overline{vp}$ may be extremely sensitive to the configuration of the four pressure holes, and the discrepancy in measured $\overline{vp}$ may be due to such factor rather than the difference in the probe shape.

Acknowledgement

REFERENCES

Beaudan, P. and Moin, P., 1994, "Numerical Experiments on the Flow Past a Circular Cylinder at a Sub-Critical Reynolds Number", Technical Report, CTR Annual Research Breifs, NASA Ames/Stanford University

Ishida, T., Toyoda, K., Tao, H. and Shirahama, Y., 1995, "Study of Yaw-Angle Characteristics of Static Pressure Probe", *Proceedings of Fluids Engineering Division Conference of the Japan Society of Mechanical Engineers* (in Japanese), No. 95-19, pp. 169-170

Kravchenko, A. G. and Moin, P., 2000, "Numerical Studies of Flow over a Circular Cylinder at $Re_D = 3900$", Phys. Fluids, Vol. 12, pp. 403-417

Kawata T., Naka, Y., Fukagata, K. and Obi, S., 2011, "Simultaneous Measurement of Velocity and Fluctuating Pressure in a Turbulent Wing-Tip Vortex Using Triple Hot-Film Sensor and Miniature Total Pressure Probe", Flow Turbulence Combust., Vol. 86, pp. 419-437

Lourenco, L. M. and Shih, C., "Characteristics of the Plane Turbulent near Wake of a Circular Cylinder, a Particle Image Velocimetry Study", Published in Beaudan and Moin (1994)

Mitta, R. and Moin, P., 1997, "Suitability of Upwind-Biased Finite-Difference Schemes for Large-Eddy Simulation of Turbulent Flows", AIAA J. Vol. 35, 1415

Naka, Y., Omori, T., Obi, S. and Masuda, S., 2006, "Simultaneous Measurement of Fluctuating Velocity and Pressure in a Turbulent Mixing Layer", Int. J. Heat Fluid Flow, Vol. 27, pp. 737-746.

Naka, Y., Azegami, S., Kawata, T., Fukagata, K. and Obi, S., 2009, "Simultaneous Measurement of Velocity and Pressure in a Wing-Tip Vortex", Journal of Fluid Scienc and Technology, Vol. 4, No. 1, pp. 107-115

Ong, J. and Wallace, L., 1996, "The Velocity Field of the Turbulent Very Near Wake of a Circular Cylinder", Exp. Fluids, Vol. 20, 441

Parnaudeau, P., Carlier, J., Heitz, D., and Lamballais, E., 2008, "Experimental and Numerical Studies of the Flow over a Circular Cylinder at Reynolds Number 3900", Phys. Fluids, Vol. 20, 085101

Sakai, Y., Moriguchi, Y., Tanaka, N., Yamamoto, M., Kubo, T. and Nagata, K., 2007, "On Characteristics of Velocity and Pressure Field in Two-Dimensional Turbulent Jet", Journal of Fluid Science and Technology, Vol. 2, No. 3, pp. 611-622

Toyoda, K., Okamoto, T. and Shirahama, Y., 1994, "Eduction of Vortical Structures by Pressure Measurements in Noncircular Jets", Applied Scientific Research, Vol. 53, pp. 237-248

Tsuji,Y., Fransson, J. H. M., Alfredsson, P. H. and Johansson, A. V., 2007, "Pressure Statistics and Their Scaling in High-Reynolds-Number Turbulent Boundary Layers", J. Fluid Mech., Vol. 585, pp. 1-40

Yao, Y.F., Thomas, T.G., and Sandham, N.D., 2001, "Direct Numerical Simulation of Turbulent Flow over a Rectangular Trailing Edge", Theoret. Comput. Fluid Dyn., Vol. 14, pp. 337-358